Magnetic Resonance Imaging 55 (2019) 81–85

Contents lists available at ScienceDirect

Magnetic Resonance Imaging

journal homepage: www.elsevier.com/locate/mri

Original contribution

Accelerated silent echo-planar imaging

Patrick Liebig[a,b,*], Robin M. Heidemann[b], Bernhard Hensel[a], David A. Porter[c]

[a] Cent. of Med. Phys. and Biomed. Eng., Friedrich-Alexander-Univ. Erlangen-Nürnberg, Erlangen, Germany
[b] Siemens Healthcare GmbH, Erlangen, Germany
[c] Imaging Centre of Excellence (ICE), Institute of Neuroscience and Psychology, College of Medical, Veterinary & Life Sciences University of Glasgow, Glasgow, United Kingdom

ARTICLE INFO

Keywords:
EPI
Parallel imaging
Non-Cartesian
Iterative reconstruction
Acoustic noise
Interlaced FT

ABSTRACT

Purpose: The standard approach to Echo-Planar Imaging (EPI) is to use trapezoidal readout (RO) gradients with blipped phase-encoding (PE) gradients. Sinusoidal RO gradients with constant PE gradients can reduce acoustic noise. However, this sequence, originally introduced by Mansfield et al., constitutes major challenges for Cartesian parallel imaging techniques. In this study two alternatives to reconstruct a non-blipped EPI are proposed and evaluated.

Theory and methods: The first method separates the acquired k-space data into odd and even echoes and applies Cartesian GRAPPA separately to each partial data set. Afterwards, the resulting reconstructed data sets for each echo are summed in image space. In the second method, an iterative parallel-imaging algorithm is used to reconstruct images from the highly non-Cartesian data samples.

Results: Compared to blipped-EPI, the first method reduces image SNR depending on the acceleration factor between 11% and 60%. For an acceleration factor of 3 folding artefacts appear. The second method produces slight fold-over artefacts although image SNR is on the same level as the blipped approach.

Conclusion: In this study, we have introduced two new approaches to EPI that allow the use of Cartesian parallel imaging in conjunction with continuous data sampling. In addition to providing a reduction in acoustic noise compared to the standard blipped PE EPI sequence, the proposed techniques improve sampling efficiency, resulting in a reduction of the echo-spacing. Of the two methods, the second approach, based on an iterative image reconstruction, provides higher SNR, but requires a longer reconstruction time.

1. Introduction

Since its introduction by Mansfield in 1977, the original echo-planar imaging (EPI) sequence [1] has been adapted to improve image quality and to make use of advanced gradient systems. Its high imaging speed makes it a core methodology for providing high temporal resolution in functional magnetic resonance imaging (fMRI) [2] and for reducing motion-induced image artefacts in diffusion magnetic resonance imaging (dMRI) [3]. The drawback of EPI is a high level of acoustic noise during the examinations of up to 138 dB [4]. Although in a typical setting values of around 100 dB are more common [5]. This noise level is a discomfort to the subject being scanned and can be a severe disruption to fMRI studies, because it impedes communication with the subject; it also contributes a high level of auditory stimulation, which is especially problematic for studies of the auditory system itself [6]. Beside the auditory system, the visual and motor systems can also be influenced by acoustic noise [7].

Several procedures to reducing acoustic noise during fMRI examinations have been proposed, which range from hardware modifications [8–10] and gradient waveform modifications [11–15] to special sampling strategies [16–18]. Today, it is standard practice to perform EPI using trapezoidal readout (RO) gradients and blipped phase-encoding (PE) gradients. Although this is technically convenient on modern scanners, acoustic noise can be reduced by going back to the original form of the EPI sequence introduced by Mansfield; this uses a sinusoidal RO gradient that has a narrow frequency band that allows acoustic resonance frequencies of the gradient system to be effectively avoided [14]. When combined with blipped phase-encoding (PE) gradients, the sinusoidal gradient waveform can be used with Cartesian parallel imaging techniques [15]. This results in a noise reduction of up to 11 dB compared to standard EPI with blipped PE gradients and a trapezoidal RO gradient waveform. However, it has also been shown that blipped PE gradients make a significant contribution to acoustic noise [15].

* Corresponding author at: Diagnostic Imaging, SHS DI MR RCT, Allee am Roethelheimpark 2, 91052 Erlangen, Germany.
E-mail address: patrick.liebig@siemens-healthineers.com (P. Liebig).

https://doi.org/10.1016/j.mri.2018.09.016
Received 4 May 2018; Received in revised form 13 September 2018; Accepted 16 September 2018

Indeed, the quietest EPI sequence is the original one introduced by Mansfield [1] with a constant PE gradient and a noise reduction of 20 dB compared to the standard EPI with blipped phase encoding [14]. However, a straightforward, two dimensional fast Fourier transform (2D-FFT) cannot be used with this data sampling scheme due to the non-Cartesian zigzag-style trajectory. To process data acquired in this way, a different reconstruction procedure, the interlaced Fourier transform (iFT), was introduced by Sekihara in 1987 [19]. It was already shown by Schmitter et al. [14] that this sequence reconstructed with the iFT has a beneficial effect upon fMRI studies. This was more extensively investigated by Pelle et al. [20] who showed that in all areas except for the frontal ones the quiet EPI sequence with a sinusoidal RO and a constant PE gradient is superior to the standard trapezoidal one. Although, as mentioned in this paper, no Cartesian parallel imaging techniques could be applied due to the non-Cartesian trajectory. As a result of the longer RO train, compared to the standard trapezoidal EPI sequence, a significant signal dropout in the frontal areas occurs along with a lower activation level.

In a first approach, we use a slightly modified version of the original EPI sequence by Mansfield to achieve a pure zigzag trajectory without deviations. This makes it possible to apply Cartesian parallel imaging methods by processing odd and even echoes separately. In a second approach, we use the original EPI sequence with a constant PE gradient in combination with non-Cartesian iterative parallel imaging methods, such as ESPIRiT [21]. We also show that we can reconstruct this non-Cartesian trajectory with Cartesian parallel imaging methods. Finally, we compare these two types of reconstruction methods to the iFT.

2. Methods

2.1. Sequence timing

In EPI with blipped PE and sinusoidal RO gradients (see Fig. 1A), the resulting k-space trajectory shows equidistant sampling along the PE direction, but non-equidistant sampling along the RO direction. In this case, a simple one-dimensional regridding of the data is sufficient to align them onto a Cartesian grid. When the blipped PE is replaced by a constant PE gradient, as proposed originally, the resulting k-space trajectory is a sinusoidal zigzag (see Fig. 1B). A true zigzag trajectory without deviations can be realized by using a variable low amplitude gradient waveform that is the modulus of the RO gradient. This sequence is called Zigzag-Aligned-Projections (ZAP) PE EPI [22] (see Fig. 1C). Both of these methods can be combined with either a trapezoidal or sinusoidal RO gradient. However, in this work, only the sinusoidal case is considered.

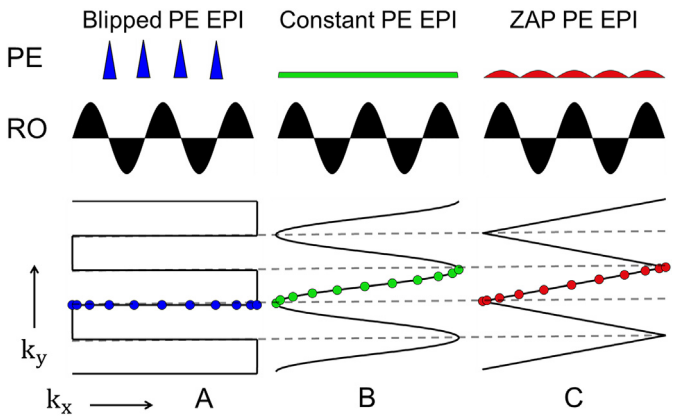

Fig. 1. Sinusoidal EPI with (A) blipped PE, (B) constant PE and (C) ZAP PE. Note, that there is non-equidistant sampling along the RO direction in all three cases.

2.2. Image reconstruction

For the reconstruction of data acquired with zigzag trajectories (constant PE and ZAP PE EPI), some of the standard EPI reconstruction steps can be applied: these include phase correction for the temporal misalignment of odd and even echoes and standard 1D-Kaiser-Bessel-regridding along the RO direction for sinusoidal RO gradients [23]. These steps were performed within the manufacturer's proprietary image calculation environment (ICE, Siemens Healthcare, Erlangen, Germany). However, due to the non-Cartesian nature of these data in two dimensions, it is not possible to use well established Cartesian parallel imaging methods, such as Sensitivity Encoding (SENSE) [24] or Generalized Autocalibrating Partially Parallel Acquisitions (GRAPPA) [25]. This paper is focused on the GRAPPA technique, but the general concepts can be applied to other parallel imaging approaches. To overcome this limitation, the zigzag-sampled data in this study were reconstructed using three alternative approaches: (1) an interlaced Fourier Transform (iFT) algorithm [19], (2) a modified Cartesian GRAPPA procedure, and (3) an iterative reconstruction method using the ESPIRiT method [21]. All approaches were implemented offline in MATLAB (The Mathworks, Natick, MA, USA). The ESPIRiT technique was applied using version 0.4.01 of the BART reconstruction toolbox [26].

2.3. Interlaced Fourier transform

For our implementation of the iFT [19], we use an improved method as described in [27]. Interlacing is performed in the phase-encoding direction using two data sets derived from the odd and even echoes respectively. The trajectories for the odd and even echoes are shifted in the PE direction relative to each other. This means that for a given data column along the PE direction, considering all acquired data for both odd and even echoes, there are two sampling step sizes. One step size fulfills the Nyquist sampling criterion and one does not. According to the general sampling theorem by Papoulis [28], it is possible to reconstruct alias-free images even if the Nyquist criterion is not fulfilled everywhere in k-space, as long as the Nyquist criterion is fulfilled on average. This is the case for the zigzag trajectory, except for the data points at the edges. Due to this, 18% of the data in the RO direction at the edges are skipped and the remaining 82% are used for image reconstruction. This is equivalent to the sampling window used in the standard blipped EPI case. Therefore no difference between constant PE EPI and blipped PE EPI exists concerning the sampling window.

2.4. Reconstruction using modified GRAPPA

After acquisition, the k-space data for odd and even echoes are separated. Cartesian GRAPPA reconstruction is applied to each of the separated k-space data sets resulting in two complete data sets with Nyquist sampling, thereby not affected by aliasing (shown in Fig. 2). The separated data sets have a reduction factor that is twice as large as the acceleration factor. However, only the g-factor induced losses are higher compared to standard blipped PE EPI and Cartesian GRAPPA reconstruction. The resulting two k-space trajectories have opposite slopes, which would result in two images that are tilted with respect to each other. This is corrected by regridding the separated data sets onto a Cartesian grid using Kaiser-Bessel gridding with a kernel width of four. The resulting two magnitude images are summed in image space. Alternatively one could correct the shearing by a linear phase correction according to the Fourier Shift Theorem.

It should be noted that this approach is strictly speaking only valid for ZAP PE EPI. In constant PE EPI there are sinusoidal deviations from a perfect zigzag trajectory (compare Fig. 1). However, these deviations are in general very small and therefore this modified GRAPPA approach can also be applied to constant PE EPI and not only to ZAP PE EPI.

For GRAPPA, the acquisition of a small subset of Nyquist-sampled,

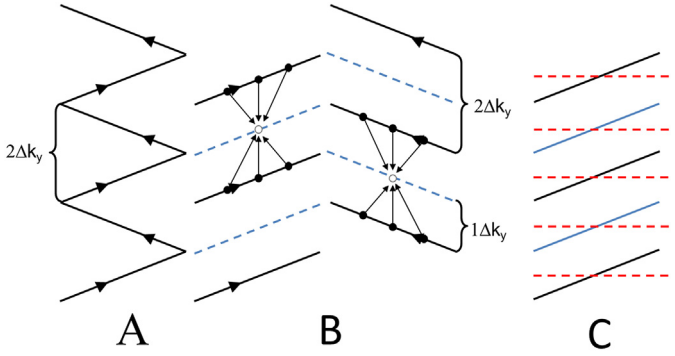

Fig. 2. Non-accelerated k-space trajectory (A). Application of GRAPPA to separate k-space data for odd and even echoes (B) and subsequent gridding onto Cartesian grid (C, shown only for odd echoes).

k-space data is necessary. The data from this non-accelerated acquisition, the so named Auto-Calibration Signal (ACS), are used to determine the GRAPPA reconstruction weights, which are later used to reconstruct missing data in an accelerated scan.

For this modified GRAPPA approach, we have to apply GRAPPA in a sheared k-space. Therefore, in a first approach, we match the slope of the acquired ACS k-space data lines to the slope of the acquired accelerated k-space lines. Due to the opposite slopes of odd and even echoes, we therefore have to acquire two sets of ACS data, one for the odd echoes and one for the even echoes. During our investigations, it was observed that standard blipped PE EPI ACS data, or non-sheared ACS data, can be used to generate GRAPPA reconstruction weights without obvious detrimental effect compared to a sheared ACS acquisition with a matched slope. Since there is no obvious benefit in using ACS data with a matched slope, we use the simpler approach of an ACS acquisition based on standard EPI. It would also be possible to acquire ACS data using the FLEET [29] or FLASH ACS [30] methods, which have been shown to give higher temporal SNR than with an EPI-based ACS scan.

For all experiments, the number of ACS lines was 12 times the reduction factor (R). For zigzag EPI, R is equivalent to the undersampling factor in the separated k-spaces, while the acceleration factor (AF) is the undersampling of the complete zigzag data set. This means R is twice as large as AF for zigzag acquisitions. As a side effect of the separation, it is not necessary to apply a phase correction, because in each data set we only have odd or even echoes.

2.5. Image acquisition

Experiments were performed on a 7T MAGNETOM Terra whole-body MR scanner (Siemens Healthcare, Erlangen, Germany). One healthy subject was examined with a 32-channel Head Coil (Nova Medical, USA) and informed consent was obtained before the study.

For comparison, all images were gridded onto the same Cartesian grid as described in the Section 2.4. To measure the SNR, an oil phantom was acquired twice with the exact same parameters, as used for the invivo scans. These two images were afterwards substracted to generate a noise only image. From there on the SNR was calculated. This was performed for 20 different regions of interest as described in [31]. This method provides reasonable results for phantom experiments using phased array coils and parallel imaging.

2.6. Verification of the efficiency gain

Calculation of sequence timing was performed using the IDEA pulse sequence development environment (Siemens Healthcare, Erlangen, Germany) configured for a MAGNETOM Skyra. The first initial measurements were performed on a Skyra system, but later a Terra system was used. Therefore, the simulations are on the Skyra and the actual measurements took place on the Terra. The calculations were used to investigate the possible gain in efficiency provided by continuous data sampling, compared to the case when data sampling is paused during the PE gradients in blipped PE EPI. Here efficiency means what minimal FOV can be reached for a given parameter set. The smaller the minimum possible FOV, the better the gradient performance, or in other

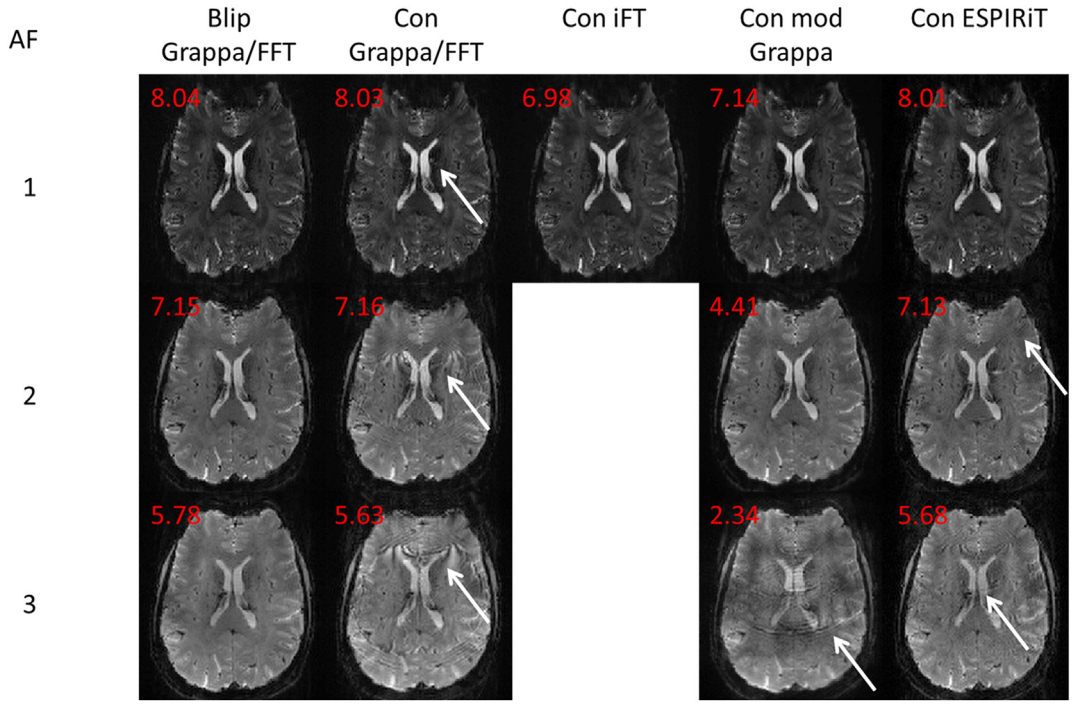

Fig. 3. Images acquired at 7T with blipped PE EPI (A) and Constant PE EPI (B-E) and reconstructed with standard Cartesian 2D-FFT/GRAPPA (A,B), the suggested modified GRAPPA approach (D), ESPIRiT with a calibration size of 20 × 20 (E) and iFT (C). Data are shown for acceleration factor s of 1 (top row) to 3 (bottom row). The protocol for these images is very similar: FOV 192 × 192 mm^2; Matrix 128 × 128; TE 48/27/20 ms; TR 1000 ms; Nominal Flip Angle 70°.

words the more efficient is the applied sequence. In detail the efficiency is defined as: $\frac{minFOV_B - minFOV_C}{minFOV_B}$, where the subscripts B and C stand for blipped and continuous sampling respectively. The protocol for blipped PE EPI (Fig. 3) was set to a matrix size of 100 with echo-spacings ranging from 0.52 ms to 1.0 ms.

3. Results

3.1. In vivo images

All in vivo images were acquired with a sinusoidal RO gradient. Fig. 3 shows images acquired in vivo with constant PE EPI and reconstructed with the proposed GRAPPA approach, ESPIRiT, iFT and standard GRAPPA. SNR values are shown in red. Similar results were seen with images acquired with ZAP EPI; these images have not been shown, but can be seen elsewhere [22]. The iFT method produces artefact-free images for the non-accelerated case with a slightly reduced SNR (6.98). For the non-accelerated acquisitions, the SNR of the modified GRAPPA approach (7.14) is 11% lower than that of blipped PE EPI with standard GRAPPA reconstruction (8.04). For the twofold accelerated acquisitions the SNR of Constant PE EPI in conjunction with modified GRAPPA (4.41) is 38% lower than the SNR for the blipped PE EPI approach (7.15). The threefold accelerated acquisition exhibit strong aliasing artefacts with a 60% lower SNR. This is due to the fact that the reduction factor for the separated odd and even echo data sets is twice the acceleration factor (Fig. 4). The images reconstructed with ESPIRiT give comparable SNR with slight artefacts. However, as can be seen in Fig. 3, a straightforward application of 2D-FFT/GRAPPA to a zigzag trajectory gives high frequency artefacts and blurring in the image (indicated by arrows).

3.2. Gain in efficiency

Fig. 5 shows that there is an increase in efficiency for continuous sampling compared to blipped sampling for higher acceleration factors and lower echo-spacings. The values range from 0.5% to 7.6%, depending on the duration of the original sampling window compared to the continuous one. The relative gain in efficiency increases with decreasing echo-spacing or increasing blip duration. For example, for an echospacing of 0.36 ms, the gain in efficiency for a three-fold accelerated acquisition is at 9.8%. This echospacing is usually accomplished by a RO segmented multishot approach [32]. The same is true for interleaved EPI [33], where the blips are getting greater and thereby longer. In that case, the gain in efficiency for 4 interleaves with an acceleration factor of 3 is 8.14%.

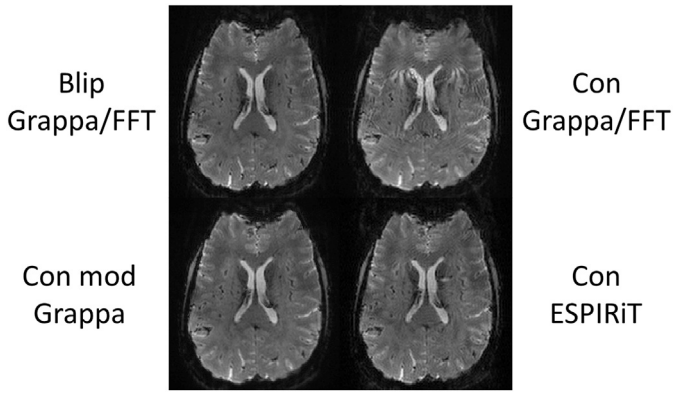

Fig. 4. Zoomed images with acceleration factor equal to 2. Top left: image acquired with blipped PE EPI and reconstructed with 2D FFT. Top right: image acquired with constant PE EPI and reconstructed with 2D FFT. Bottom left: image acquired with constant PE EPI and reconstructed with the modified GRAPPA method described in the text. Bottom right: image acquired with constant PE EPI and reconstructed using the ESPIRiT method.

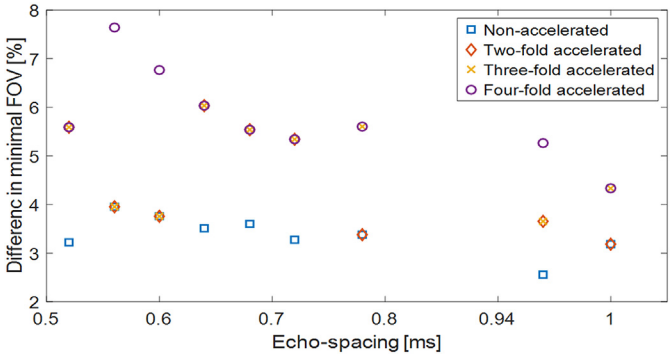

Fig. 5. Efficiency as defined by the difference in minimum possible FOV (compare Section 2.6) is shown for a range of echo-spacings and acceleration factors. The data show the gain in efficiency that can be provided by continuous sampling scheme compared to that of blipped PE EPI.

4. Discussion and conclusion

In this paper, we introduced a reconstruction method that allows Cartesian parallel imaging techniques (e.g. GRAPPA) to be used with zigzag EPI trajectories. Furthermore, we also investigated iterative reconstruction (e.g. ESPIRiT) for data acquired on a zigzag trajectory. Zigzag EPI sequences generate a lower acoustic noise, regardless of the RO gradient, than standard blipped PE EPI; this especially is beneficial for fMRI studies. When combined with either Cartesian or iterative parallel imaging methods, the efficiency is increased. This is because continuous sampling throughout the RO train is now possible. Finally, we compared our reconstruction methods to the interlaced Fourier Transformation (iFT), which is the reference method for reconstructing data sampled using zigzag k-space trajectories.

The iFT algorithm gives artefact-free images for non-accelerated acquisitions. However, it cannot be combined with accelerated acquisitions. By using Cartesian GRAPPA with zigzag trajectories, the SNR compared to a 2D-FFT is lower due to increased g-factor losses. This becomes even more prominent for accelerated scans, because then there is a factor of two, due to the separation of k-spaces, in addition to the standard acceleration factor. One advantage of our approach is that phase correction is not required to correct differences between odd and even echoes, which is similar to the method from Kellman et al. that also uses parallel imaging methods to reduce ghosting in EPI [34].

Another approach to image reconstruction is iterative parallel imaging like ESPIRiT. The SNR is higher and only minor artefacts are visible compared to reconstructing zigzag data with Cartesian GRAPPA. This is not necessarily intuitive as for an acceleration factor of 3 the edges of k-space are already 6-fold undersampled. With a 32-channel head-coil it is generally difficult to successfully reconstruct a data set, which is 6-fold undersampled along one direction. As a drawback of this method, a nine-fold longer time is required (47 s per slice), for image reconstruction compared to Cartesian GRAPPA.

To summarize this, up to an acceleration factor of 2 ESPIRiT and odd-even GRAPPA give good results. For an acceleration factor of 3, only reconstructions with ESPIRiT result in acceptable image quality. For higher acceleration factors, remaining fold-over artefacts are severe. So a factor of 3 is the current limit of the proposed method. The suggested odd-even GRAPPA technique can only be applied to zigzag trajectories. It therefore represents a way to reconstruct a non-Cartesian trajectory (zigzag) with a Cartesian reconstruction by reordering the data (odd-even) into a Cartesian k-space. This approach is similar to the methods suggested by [35–40].

For zigzag EPI sequences we expect a slightly higher efficiency compared to the blipped sequence due to the continuous sampling

during the readout echo train. With standard blipped PE EPI, data sampling is suspended during the blips. The increased efficiency of zigzag EPI can make it possible to image with a shorter RO train when compared to the same scan protocol with blipped PE EPI. As shown in Fig. 5, the gain in efficiency improves significantly as the echo spacing is reduced, making the zigzag EPI methods of particular interest for multi-shot EPI using readout segmentation [32]. There are also potential benefits for interleaved acquisitions [33], which typically use larger blipped PE gradients.

Acoustic Noise measurements have been performed in the literature for the difference between a blipped and a constant PE approach [27]. It has been shown that the PE blips contribute between 3 and 7 dB to the overall acoustic noise level. Another aspect is that the human ear is more sensitive to certain frequencies and thereby making the effect of the acoustic noise onto the volunteer a function of the applied frequency. Gradient blips are at twice the frequency of the RO gradient. Thereby the resulting sound has very high frequency components where the human ear is in general more sensitive.

In summary, we have introduced a new reconstruction method, which allows Cartesian GRAPPA to be used on non-Cartesian zigzag data in EPI. Furthermore, we have explored the idea of using non-Cartesian parallel imaging techniques for zigzag trajectories to reduce acoustic noise and increase the efficiency compared to blipped PE EPI. As a result, the originally proposed EPI sequence by Mansfield with constant PE or ZAP PE EPI, as a slightly modified version, can be directly used in conjunction with parallel imaging as an efficient EPI sequence with reduced acoustic noise. Future work will extend zigzag EPI methods to multi-shot EPI sequences and multiband acquisitions such as blipped-CAIPI [41].

Acknowledgements

We would like to thank Dr. Sebastian Schmitter and Dr. Mario Zeller for very helpful discussions. Regarding DAP's contribution to this work, the Imaging Centre of Excellence at the University of Glasgow is supported by a gift from the Sackler Trust and the Dr. Mortimer and Theresa Sackler Foundation and also received financial support from the Wolfson Foundation.

References

[1] Mansfield P. Multi-planar image formation using NMR spin echoes. J Phys C Solid State Phys Feb. 1977;10:L55–8.
[2] Ogawa S, et al. Intrinsic signal changes accompanying sensory stimulation: functional brain mapping with magnetic resonance imaging. Proc Natl Acad Sci U S A Jul. 1992;89(13):5951–5.
[3] Turner R, Le Bihan D, Chesnick AS. Echo-planar imaging of diffusion and perfusion. Magn Reson Med Jun. 1991;19(2):247–53.
[4] Ravicz ME, Melcher JR, Kiang NY-S. Acoustic noise during functional magnetic resonance imaging. J Acoust Soc Am Oct. 2000;108(4):1683–96.
[5] Miyati T, et al. Acoustic noise analysis in echo planar imaging: multicenter trial and comparison with other pulse sequences. IEEE Trans Med Imaging Aug. 1999;18(8):733–6.
[6] Bandettini PA, Jesmanowicz A, Van Kylen J, Birn RM, Hyde JS. Functional MRI of brain activation induced by scanner acoustic noise. Magn Reson Med Mar. 1998;39(3):410–6.
[7] Cho ZH, Chung SC, Lim DW, Wong EK. Effects of the acoustic noise of the gradient systems on fMRI: a study on auditory, motor, and visual cortices. Magn Reson Med Feb. 1998;39(2):331–5.
[8] Katsunuma A, Takamori H, Sakakura Y, Hamamura Y, Ogo Y, Katayama R. Quiet MRI with novel acoustic noise reduction. Magma N Y N Jan. 2002;13(3):139–44.
[9] Mansfield P, Haywood B. Principles of active acoustic control in gradient coil design. Magma Magn Reson Mater Phys Biol Med Jun. 2000;10:147–51.
[10] Cho ZH, et al. A new silent magnetic resonance imaging using a rotating DC gradient. Magn Reson Med Feb. 1998;39(2):317–21.
[11] Hennel F, Girard F, Loenneker T. 'Silent' MRI with soft gradient pulses. Magn Reson Med Jul. 1999;42(1):6–10.
[12] Tomasi DG, Ernst T. Echo planar imaging at 4 Tesla with minimum acoustic noise. J Magn Reson Imaging JMRI Jul. 2003;18(1):128–30.
[13] Oesterle C, Hennel F, Hennig J. Quiet imaging with interleaved spiral read-out. Magn Reson Imaging Dec. 2001;19(10):1333–7.
[14] Schmitter S, Diesch E, Amann M, Kroll A, Moayer M, Schad LR. Silent echo-planar imaging for auditory FMRI. Magma N Y N Sep. 2008;21(5):317–25.
[15] Zapp J, Schmitter S, Schad LR. Sinusoidal echo-planar imaging with parallel acquisition technique for reduced acoustic noise in auditory fMRI. J Magn Reson Imaging JMRI Sep. 2012;36(3):581–8.
[16] Hall DA, et al. 'Sparse' temporal sampling in auditory fMRI. Hum Brain Mapp 1999;7(3):213–23.
[17] Scheffler K, Bilecen D, Schmid N, Tschopp K, Seelig J. Auditory cortical responses in hearing subjects and unilateral deaf patients as detected by functional magnetic resonance imaging. Cereb Cortex N Y N 1991 Mar. 1998;8(2):156–63.
[18] Amaro EJ, et al. Acoustic noise and functional magnetic resonance imaging: current strategies and future prospects. J Magn Reson Imaging JMRI Nov. 2002;16(5):497–510.
[19] Sekihara K, Kohno H. New reconstruction technique for echo-planar imaging to allow combined use of odd and even numbered echoes. Magn Reson Med Nov. 1987;5(5):485–91.
[20] Peelle JE, Eason RJ, Schmitter S, Schwarzbauer C, Davis MH. Evaluating an acoustically quiet EPI sequence for use in fMRI studies of speech and auditory processing. NeuroImage Oct. 2010;52(4):1410–9.
[21] Uecker M, et al. ESPIRiT–an eigenvalue approach to autocalibrating parallel MRI: where SENSE meets GRAPPA. Magn Reson Med Mar. 2014;71(3):990–1001.
[22] Liebig P, Heidemann RM, Porter DA. Zigzag-aligned-projections in echo-planar imaging. Presented at the Annual Meeting ISMRM, Singapore, vol. 24. 2016.
[23] Jackson JI, Meyer CH, Nishimura DG, Macovski A. Selection of a convolution function for Fourier inversion using gridding [computerised tomography application]. IEEE Trans Med Imaging 1991;10(3):473–8.
[24] Pruessmann KP, Weiger M, Scheidegger MB, Boesiger P. SENSE: sensitivity encoding for fast MRI. Magn Reson Med Nov. 1999;42(5):952–62.
[25] Griswold MA, et al. Generalized autocalibrating partially parallel acquisitions (GRAPPA). Magn Reson Med Jun. 2002;47(6):1202–10.
[26] Uecker M, Tamir J, Ong F, Holme C, Lustig M. Bart: Version 0.4.01. Zenodo; 23-Jun-2017.
[27] Schmitter S. Entwicklung von geräuscharmen Bildgebungstechniken für die funktionelle Magnetresonanztomographie. 2008. p. 10. 169 S.
[28] Papoulis A. Generalized sampling expansion. IEEE Trans Circuits Syst Nov. 1977;24(11):652–4.
[29] Polimeni JR, et al. Reducing sensitivity losses due to respiration and motion in accelerated echo planar imaging by reordering the autocalibration data acquisition. Magn Reson Med Feb. 2016;75(2):665–79.
[30] Talagala SL, Sarlls JE, Liu S, Inati SJ. Improvement of temporal signal-to-noise ratio of GRAPPA accelerated EPI using a FLASH based calibration scan. Magn Reson Med Jun. 2016;75(6):2362–71.
[31] Firbank MJ, Coulthard A, Harrison RM, Williams ED. A comparison of two methods for measuring the signal to noise ratio on MR images. Phys Med Biol Dec. 1999;44(12):N261–4.
[32] Porter DA, Heidemann RM. High resolution diffusion-weighted imaging using readout-segmented echo-planar imaging, parallel imaging and a two-dimensional navigator-based reacquisition. Magn Reson Med Aug. 2009;62(2):468–75.
[33] McKinnon GC. Ultrafast interleaved gradient-echo-planar imaging on a standard scanner. Magn Reson Med Nov. 1993;30(5):609–16.
[34] Kellman P, McVeigh ER. Phased array ghost elimination. NMR Biomed May 2006;19(3):352–61.
[35] Griswold M, Heidemann RM, Jakob PM. Direct parallel imaging reconstruction of radially sampled data using GRAPPA with relative shifts. Proceedings of the 11th Annual Meeting of ISMRM, Toronto, Canada 2003. p. 2349.
[36] Heidemann RM, et al. Direct parallel image reconstructions for spiral trajectories using GRAPPA. Magn Reson Med Aug. 2006;56(2):317–26.
[37] Heberlein K, Hu X. Auto-calibrated parallel spiral imaging. Magn Reson Med Mar. 2006;55(3):619–25.
[38] Heidemann RM, et al. Fast method for 1D non-cartesian parallel imaging using GRAPPA. Magn Reson Med Jun. 2007;57(6):1037–46.
[39] Breuer FA, et al. Zigzag sampling for improved parallel imaging. Magn Reson Med Aug. 2008;60(2):474–8.
[40] Skare S, Newbould RD, Nordell A, Holdsworth SJ, Bammer R. An auto-calibrated, angularly continuous, two-dimensional GRAPPA kernel for propeller trajectories. Magn Reson Med Dec. 2008;60(6):1457–65.
[41] Setsompop K, Gagoski BA, Polimeni JR, Witzel T, Wedeen VJ, Wald LL. Blipped-controlled aliasing in parallel imaging for simultaneous multislice echo planar imaging with reduced g-factor penalty. Magn Reson Med Aug. 2011;67(5):1210–24.